EUKARYOTIC CELL, Mar. 2007, p. 398–412 Vol. 6, No. 3
1535-9778/07/$08.00+0 doi:10.1128/EC.00357-06


# Molecular Cloning of Apicoplast-Targeted *Plasmodium falciparum* DNA Gyrase Genes: Unique Intrinsic ATPase Activity and ATP-Independent Dimerization of PfGyrB Subunit▽†

Mohd Ashraf Dar,[1] Atul Sharma,[1] Neelima Mondal,[2] and Suman Kumar Dhar[1]*

*Special Centre for Molecular Medicine,[1] and School of Life Sciences,[2] Jawaharlal Nehru University, New Delhi 110067, India*

Received 10 November 2006/Accepted 20 December 2006

**DNA gyrase, a typical type II topoisomerase that can introduce negative supercoils in DNA, is essential for replication and transcription in prokaryotes. The apicomplexan parasite *Plasmodium falciparum* contains the genes for both gyrase A and gyrase B in its genome. Due to the large sizes of both proteins and the unusual codon usage of the highly AT-rich *P. falciparum gyrA* (Pf*gyrA*) and Pf*gyrB* genes, it has so far been impossible to characterize these proteins, which could be excellent drug targets. Here, we report the cloning, expression, and functional characterization of full-length PfGyrB and functional domains of PfGyrA. Unlike *Escherichia coli* GyrB, PfGyrB shows strong intrinsic ATPase activity and follows a linear pattern of ATP hydrolysis characteristic of dimer formation in the absence of ATP analogues. These unique features have not been reported for any known gyrase so far. The Pf*gyrB* gene complemented the *E. coli* gyrase temperature-sensitive strain, and, together with the N-terminal domain of PfGyrA, it showed typical DNA cleavage activity. Furthermore, PfGyrA contains a unique leucine heptad repeat that might be responsible for dimerization. These results confirm the presence of DNA gyrase in eukaryotes and confer great potential for drug development and organelle DNA replication in the deadliest human malarial parasite, *P. falciparum*.**

DNA topoisomerases are a special class of enzymes that promote the interconversions of various topological forms of DNA that are generated during DNA replication, transcription, recombination, or related processes (8, 12). These enzymes are grouped mainly into two classes, namely, type I and type II, based on their ability to break one or both strands of DNA. Type II enzymes are further divided into A and B subclasses. The archaeon *Sulfolobus shibatae* contains structurally distinct type IIB topoisomerases (8). Eukaryotic type IIA topoisomerases form homodimers, whereas bacterial type IIA enzymes form heterotetramers comprised of two subunits of A and B polypeptides each (8).

The DNA gyrase falls into the type IIA category, and it is responsible for catalyzing ATP-dependent DNA supercoiling activity in prokaryotes (22, 31). The best-studied gyrase so far is from *Escherichia coli*, which forms an $A_2B_2$ complex. The GyrA N-terminal domain contains the DNA breakage and union domain, while the C-terminal domain shows DNA wrapping activity (41, 42). The GyrB N-terminal domain has an ATPase function, whereas the C-terminal domain binds to DNA and probably interacts with GyrA (6, 9, 21). These enzymes are excellent targets for various antibacterial agents including quinolones and coumarins (1, 16, 32, 33).

Although gyrase is commonly found in prokaryotes, there are a few recent reports of the existence of bacterium-type gyrases in plants that might be important for organellar DNA replication and transcription. It has been shown that *Arabidopsis thaliana* DNA gyrase is targeted to the chloroplast and mitochondria and that both subunits are essential for growth (51).

Similar to *Arabidopsis*, the apicomplexan parasite *Plasmodium falciparum* harbors a relict plastid or apicoplast, which possesses a 35-kb circular genome (57, 58, 59). There is phylogenetic evidence to suggest that the probable origin of the apicoplast could be due to the engulfment of photosynthetic algae by an ancient protist (4, 18, 58). This organelle became essential for cell survival at later stages of evolution due to its retention of type II fatty acid, isopentenyl diphosphate, and heme biosynthesis pathways (39). The apicoplast genome codes only for some housekeeping genes, few tRNAs, and rRNAs, and therefore, the replication and transcription processes of the apicoplast genome are dependent on nuclear-encoded apicoplast-targeted proteins (4, 20).

The nuclear genome sequence of the apicomplexan parasite *P. falciparum* contains homologues of both *gyrA* and *gyrB* in addition to topoisomerase II (4, 20). Also, the sensitivity of *P. falciparum* to ciprofloxacin provided a strong clue for the presence of these enzymes in this organism. A mammalian type II topoisomerase inhibitor could cleave both *P. falciparum* nuclear and apicoplast DNA, whereas the gyrase-specific drug ciprofloxacin could specifically cleave apicoplast DNA without affecting the nuclear DNA (17, 55).

Since malaria continues to be a major health problem globally, there is an urgent need to identify new targets for the development of novel drugs and vaccines. The apparent absence of gyrases in humans and their presence in *Plasmodium falciparum* make it an excellent target for a range of antibacterial agents. In fact, various quinolone drugs and their deriv-

* Corresponding author. Mailing address: Special Centre for Molecular Medicine, Jawaharlal Nehru University, New Delhi 110067, India. Phone: 91-11-26704559. Fax: 91-11-26161781. E-mail: skdhar2002@yahoo.co.in.

† Supplemental material for this article may be found at http://ec.asm.org/.

▽ Published ahead of print on 12 January 2007.

atives that are very potent against bacteria have also been shown to disrupt *P. falciparum* parasites (2, 3, 10, 15). However, efforts to use gyrase inhibitors to kill the parasites have been somewhat limited due to the nonavailability of recombinant enzymes from *Plasmodium falciparum* to study biochemical activity and screen inhibitors. There are no data regarding the expression of these proteins in *P. falciparum* and their targeting to the apicoplast, the organelle that is supposed to harbor these enzymes. These problems could be attributed to the fact that both *P. falciparum gyr* (Pf*gyr*) genes are relatively large (>100 kDa) and the unusual codon usage associated with the highly AT-rich sequence of *P. falciparum* (~80%). After not being able express *P. falciparum gyr* genes due to the above-mentioned problems, Khor et al. recently reported the cloning and characterization of the ATP binding domain of the *P. vivax gyrB* (Pv*gyrB*) gene, which contains ~52% AT content (30). The 43-kDa PvGyrB polypeptide shows ATPase activity that can be inhibited by the drug coumermycin. According to that study, full-length recombinant PvGyrB formed inclusion bodies, and the refolded protein was almost inactive (30). The high AT content of the *Plasmodium falciparum* genome, the unusual codon usage, and the presence of asparagine and lysine repeats within the coding region make it very difficult to work with large proteins of this organism (37). Therefore, more attempts to express only the functional domains of the relevant proteins for their biochemical characterization or to study these proteins/enzymes in related *Plasmodium* species that contain normal AT content are being made. Due to these problems, there is hardly any report in the literature of a large *Plasmodium falciparum* protein (>100 kDa) being purified under physiological conditions. However, the challenges and complexities of *P. falciparum* could not be revealed completely by studying the functionally similar enzymes/proteins in related *Plasmodium* species. Ultimately, any drug or inhibitor has to be designed against the protein from the same species that causes more fatal disease symptoms.

To investigate the biochemical and pharmacologic properties of *Plasmodium falciparum* gyrases, we took the challenge to express Pf*gyrA* and Pf*gyrB* genes by using a variety of expression systems and conditions. Here, we report for the first time the cloning, expression, and purification of full-length PfGyrB and functional domains of PfGyrA. Unlike *E. coli* GyrB (EcGyrB), PfGyrB shows intrinsic ATPase activity and follows a linear pattern of ATP hydrolysis characteristic of dimer formation in the absence of ATP analogues. This suggests that the enzyme kinetics of the protein are truly different from those of its *E. coli* counterpart. The Pf*gyrB* gene complemented the *E. coli* gyrase temperature-sensitive strain, and, together with the PfGyrA N terminal domain, it efficiently performed typical DNA cleavage activity. Both proteins are localized in the apicoplast, as shown by immunofluorescence assays. Furthermore, we have identified a hydrophobic core region that might be important for ATP-independent dimerization of PfGyrB. These results confirm the presence of DNA gyrases in *P. falciparum* and suggest their role in organelle replication, which could possibly be interrupted by using novel drugs against these enzymes in the future.

## MATERIALS AND METHODS

**Parasite culture and bacterial strains.** *Plasmodium falciparum* strain 3D7 was cultured in human erythrocytes in RPMI 1640 medium supplemented with 0.2% $NaHCO_3$, 10% heat-inactivated pooled human serum type A, gentamicin sulfate (10 μg/ml), and 0.2% glucose. For synchronization of the parasites, cells were treated with 5% sorbitol. Parasites were checked routinely under a microscope before harvesting. To lyse the infected erythrocytes, 0.05% saponin was used, and parasites were recovered by centrifugation (1,000 × *g*) and washed with cold phosphate-buffered saline (137 mM NaCl, 2.7 mM KCl, 10 mM $Na_2HPO_4$, 2 mM $KH_2PO_4$, pH 7.4) (34).

*E. coli* strain DH10B was used for cloning purposes. BL21 Codon Plus and BLR(DE3) cells were used for the expression of the recombinant proteins. *E. coli* strains KNK453 [*E. coli gyrA*(Ts)] and N4177 [*E. coli gyrB*(Ts)] were used for the complementation assay. The details of these strains are listed in Table S1 in the supplemental material.

**DNA manipulations.** *Plasmodium falciparum gyrA* and *gyrB* genes were amplified by PCR using *Pfu* DNA polymerase (Stratagene), *P. falciparum* strain 3D7 genomic DNA as a template, and specific primer sets (P8 and P9 for Pf*gyrA* and P1 and P2 for Pf*gyrB*) (see Table S2 in the supplemental material) (49). The details of the cloning of the full-length and different deletion and point mutant forms of Pf*gyrA*, Pf*gyrB*, and the *E. coli* counterparts for protein expression and complementation studies are discussed in the supplemental material. All relevant primers are shown in Table S2 in the supplemental material.

The Pf*ACP* gene was amplified by reverse transcription (RT)-PCR using the specific primers P25 and P26 (see Table S2 in the supplemental material), cloned into BamHI and XhoI sites of plasmid pGEX6P2, and subsequently sequenced.

**RNA extraction and RT-PCR analysis.** Total RNA was isolated from the infected erythrocytes at different stages by using TRIzol reagent (Life Technologies) according to the protocol supplied by the vendor. The RT product was made by using an Invitrogen kit according to the manufacturer's instructions. The RT products were subsequently used for PCR using the specific primers P11 and P12 for Pf*gyrA* and P1 and P4 for Pf*gyrB*. For a loading control, RT-PCR was performed using primers P23 and P24 for Pf*GAPDH*. All primers are shown in Table S2 in the supplemental material.

**Protein purification, raising polyclonal antibodies, and Western blot analysis.** In order to purify the fusion proteins, *Escherichia coli* strain BL21 Codon Plus or BLR(DE3) was transformed with pET28a recombinant plasmid constructs. Several conditions were optimized for the purification of wild-type and mutant forms of PfGyr and EcGyr proteins. The details of the protein purification methods (including glutathione *S*-transferase [GST]-*P. falciparum* acyl carrier protein [ACP]) are described in the supplemental material.

Protein concentrations were determined by the Bradford method (Bio-Rad kit), according to the instructions of the vendor, by using bovine serum albumin (BSA) as a standard.

Polyclonal antibodies against purified $His_6$-PfGyrACC (PfGyrA coiled coil domain) and GST-PfACP were raised in mice and against $His_6$-PfGyrBC in rabbits using essentially the protocol described previously by Harlow and Lane (27). All the antibodies were later purified by affinity purification.

The fraction of the anti-GST antibodies from anti-GST-PfACP serum was separated by affinity binding to purified GST.

Western blot analysis was carried out according to standard procedures (44).

**Immunofluorescence.** Immunofluorescence assays using anti-PfGyrA, anti-PfGyrB, and anti-GST-PfACP were performed essentially as described elsewhere previously (34), with minor modifications.

**Complementation assay.** The complementarity of Pf*gyrA*/Pf*gyrB* with their *E. coli* counterparts was tested by transforming into *E. coli* strains KNK453 [*gyrA*(Ts)] and N4177 [*gyrB*(Ts)] (51), the conditional lethal mutants for *E. coli gyrA*/*gyrB* alleles, with recombinant plasmids pAD1/pAD2 and pHH3/pAG111, respectively, or pBR322 alone followed by checking the survival of *E. coli* colonies at nonpermissive temperatures (43°C and 42°C, respectively) in the presence of ampicillin and a range of IPTG (isopropyl-β-D-thiogalactopyranoside) concentrations from 0.1 mM to 0.5 mM.

**ATP hydrolysis assay.** The assay of the ATPase activity (in a 20-μl reaction mixture volume) of PfGyrB was carried out using a solution containing supercoiling buffer (containing 35 mM Tris-HCl [pH 7.5], 4 mM $MgCl_2$, 24 mM KCl, 5 mM dithiothreitol [DTT], 1.8 mM spermidine, 0.36 mg/ml BSA, and 6.5% glycerol), 1 mM ATP, 3.4 fmol of [$\gamma$-$^{32}$P]ATP, and the required amount of PfGyrB or other proteins as indicated in the figure legends (25). The reaction mixtures were incubated at 25°C for 1 h, which was followed by incubation on ice to stop the reactions. Released inorganic phosphate ($P_i$) was separated by thin-layer chromatography on a polyethylenemine cellulose strip (Sigma-Aldrich) dipped in 0.5 M LiCl and 1 M formic acid at room temperature for 1 h. The

thin-layer chromatography plate was dried, autoradiographed, and analyzed by using a phosphorimager (Fujifilm BAS-1800) for quantitation.

The coupled ATP hydrolysis (20-μl reaction mixture) in the presence of PfGyrB (wild type [WT]), PfGyrBN1, or EcGyrB43 was carried out in a reaction buffer containing 10 mM Tris-acetate (pH 7.9), 5 mM potassium acetate, 2.5 mM magnesium acetate, 2 mM DTT, and 2 mM ATP for 30 min at room temperature. The reaction was stopped by incubating the reaction mixture in a boiling water bath for 5 min. After cooling the samples to 22°C, 130 μl of a solution containing 10 mM Tris-acetate (pH 7.9), 5 mM potassium acetate, 2.5 mM magnesium acetate, 2 mM DTT, 0.5 mM phosphoenolpyruvate, 0.32 mM β-NADH, 9.8 units of pyruvate kinase, and 15.6 units of lactate dehydrogenase was added. The samples were centrifuged at 10,000 × *g* for 1 min, and the absorbance data were collected by using a Spectramax 250 microplate spectrophotometer equipped with SOFTmax software (Molecular Devices). The rate of the reaction was calculated as discussed elsewhere previously (30).

The substrate-dependent coupled ATP hydrolysis reactions were carried out as described previously (1, 45), and the absorbance data were collected by using an Ultrospec 2100 spectrophotometer (Amersham Biosciences).

**DNA cleavage and supercoiling assay.** DNA cleavage assays were carried out in a reaction buffer containing 35 mM Tris-HCl (pH 7.5), 24 mM KCl, 2 mM $CaCl_2$, 2 mM spermidine, 50 μg/ml BSA, 6.5% glycerol, 5 mM DTT, and 1.5 mM ATP in the presence of 10 μg/ml supercoiled pBR322 DNA in a total reaction mixture volume of 30 μl. The samples were incubated at 25°C for 1 h, and the reaction was terminated by the addition of 3 μl of 2% sodium dodecyl sulfate (SDS) and 1 μl of 5 mg/ml proteinase K (Sigma). Samples were further incubated at 37°C for 45 min and electrophoresed in a 1% agarose gel. The gel was finally stained with ethidium bromide. In case of quinolone-induced cleavage, 2 mM $CaCl_2$ was replaced with 4 mM $MgCl_2$ (41).

The supercoiling assays were carried out in the same buffer described above for $CaCl_2$-induced cleavage except that 4 mM $MgCl_2$ replaced 2 mM $CaCl_2$ and human Topo I (Fermentas)-treated relaxed pBR322 was used in place of supercoiled DNA (41).

**Glutaraldehyde cross-linking assay, native PAGE analysis, and gel filtration chromatography.** The cross-linking reaction was performed to stabilize the dimer/oligomer forms of the proteins, which can be distinguished from the monomer forms following SDS-polyacrylamide gel electrophoresis (PAGE) analysis. A typical cross-linking reaction buffer (20 μl) contains phosphate-buffered saline and glutaraldehyde at a final concentration of 0.001%. The samples were incubated in a 37°C water bath for 15 min and boiled at 95°C for 3 min after the addition of 3 μl SDS sample buffer and finally loaded onto a 10% SDS gel and subjected to Western blot analysis by using anti-$His_6$ antibodies (35). In the case of PfGyrBN2 and ECGyrN, the cross-linking was carried out in the presence or absence of coumermycin in a buffer containing 10 mM Tris-HCl, 100 mM KCl, 4 mM DTT, 4 mM $MgCl_2$, and 0.002% glutaraldehyde. The incubation was carried out at 25°C for 2 h. For PfGyrB (WT), incubation at 25°C for 4 h was done in the same buffer as that for PfGyrBN2. The reactions were terminated by the addition of 2× SDS sample buffer and boiling at 95°C for 3 min. The samples were loaded onto a 10% SDS-PAGE gel and subsequently subjected to Western blot analysis by using anti-$His_6$ antibodies (45). For native PAGE analysis, one microgram of each protein, as shown in Fig. 6E, was loaded onto a 10% native PAGE gel, and the proteins were resolved by using 1× Tris-borate-EDTA followed by Coomassie staining.

Wild-type PfGyrB, PfGyrBN1, or PfGyrBN2 was subjected to size-exclusion chromatography on a Pharmacia Superose-12 gel filtration column in a buffer containing 50 mM Tris-Cl (pH 7.4), 1 mM EDTA, 10 mM β-mercaptoethanol, 100 μM phenylmethylsulfonyl fluoride, 10% glycerol, and 100 mM NaCl. The column was previously calibrated using Pharmacia low- and high-molecular-weight standards as indicated on the top panel of Fig. 6H. Fractions (0.5 ml) were collected in each case. The fractions were checked for the presence of proteins by SDS-PAGE analysis.

## RESULTS

**Cloning, sequence analysis, and expression of full-length and different domains of gyrase A and gyrase B of *Plasmodium falciparum* and *E. coli*.** The *Plasmodium* Genomic Database (http://www.plasmodb.org) shows the presence of two open reading frames annotated as putative *gyrA* and *gyrB* genes (PFL1120c and PFL1915w, respectively). The PfGyrA polypeptide shows 57% homology at the N terminus and 45% homology at the C terminus, whereas the identity is 38% at the N terminus and 24% at the C terminus when compared to EcGyrA. PfGyrB overall shows 41% homology and 28% identity overall with its *E. coli* counterpart. Both polypeptides contain N-terminal extensions (~165 and ~120 amino acids, respectively) that do not show any homology with the *E. coli* gyrases. Later, using PlasmoAP and PATS prediction programs, it was found that these N-terminal sequences contain an apicoplast-targeting sequence that includes both the transit peptide as well as the signal peptide (19, 39, 40). It is likely that these enzymes are associated with the 35-kb plastid DNA replication or transcription. Putative plastid-targeting elements have been identified in the *Arabidopsis thaliana* gyrase genes (51). Transit and signal peptides might interfere with the expression and purification of these proteins from bacteria (54). Therefore, in order to clone Pf*gyrA* and Pf*gyrB* genes, PCRs were performed using 3D7 genomic DNA and specific primers (as shown in Table S2 in the supplemental material), excluding the region that contains the apicoplast-targeting sequence. Following PCR, ~2.6-kb and ~3.1-kb products were obtained for Pf*gyrB* and Pf*gyrA* genes, respectively, as shown in Fig. 1A. The PCR products were subsequently cloned into vector pET28a and sequenced completely by using overlapping primers. The deduced sequences perfectly matched the sequences reported in the database (see Fig. S1A and B in the supplemental material). The various functional domains of PfGyrA and PfGyrB are represented in the schematic diagrams (thin blocs) shown in Fig. 1B and C. The extreme N terminus of PfGyrA contains a signal peptide followed by the Topo IV domain responsible for DNA breakage and reunion. There is a unique region at the C-terminal domain that contains leucine heptad repeats that overlaps with the coiled-coil domain. This region could be involved in the dimerization of Pf*gyrA*. This region also contains a conserved GyrA C-terminal region. Interestingly, the functional C- and N-terminal domains are separated by low-complexity repeat regions not found in any other gyrases.

PfGyrB contains a signal peptide at the extreme N terminus followed by a conserved ATPase domain and a gyrase B domain separated by a low-complexity region. The C terminus contains a conserved TOPRIM domain. For analogy, we also cloned and analyzed the conserved domains of *E. coli* gyrase A and gyrase B subunits (Fig. 1D and E). The wild type and several deletion mutants were generated by PCR amplification followed by cloning in vector pET28a (Fig. 1B to D).

The expression and purification of *Plasmodium* proteins in the heterologous system are difficult due to the high AT richness of the genome and the unusual codon usage. Moreover, the situation gets worse due to the presence of asparagine and lysine repeats within the coding region (37, 43). Therefore, we decided to express full-length gyrase as well as different domains of the gyrases excluding some of these repeats. *E. coli* strain BL21 Codon Plus was transformed with all pET28a recombinant constructs, followed by the expression and purification of these proteins as $His_6$-tagged fusion proteins by essentially following the protocol described in Materials and Methods. The purified proteins were analyzed by SDS-PAGE (Fig. 1F). We were able to express and purify full-length and different domains of PfGyrB, EcGyrA, and EcGyrB (as shown in Fig. 1E). Even after extensive efforts, we were unable to express full-length PfGyrA, although we managed to express

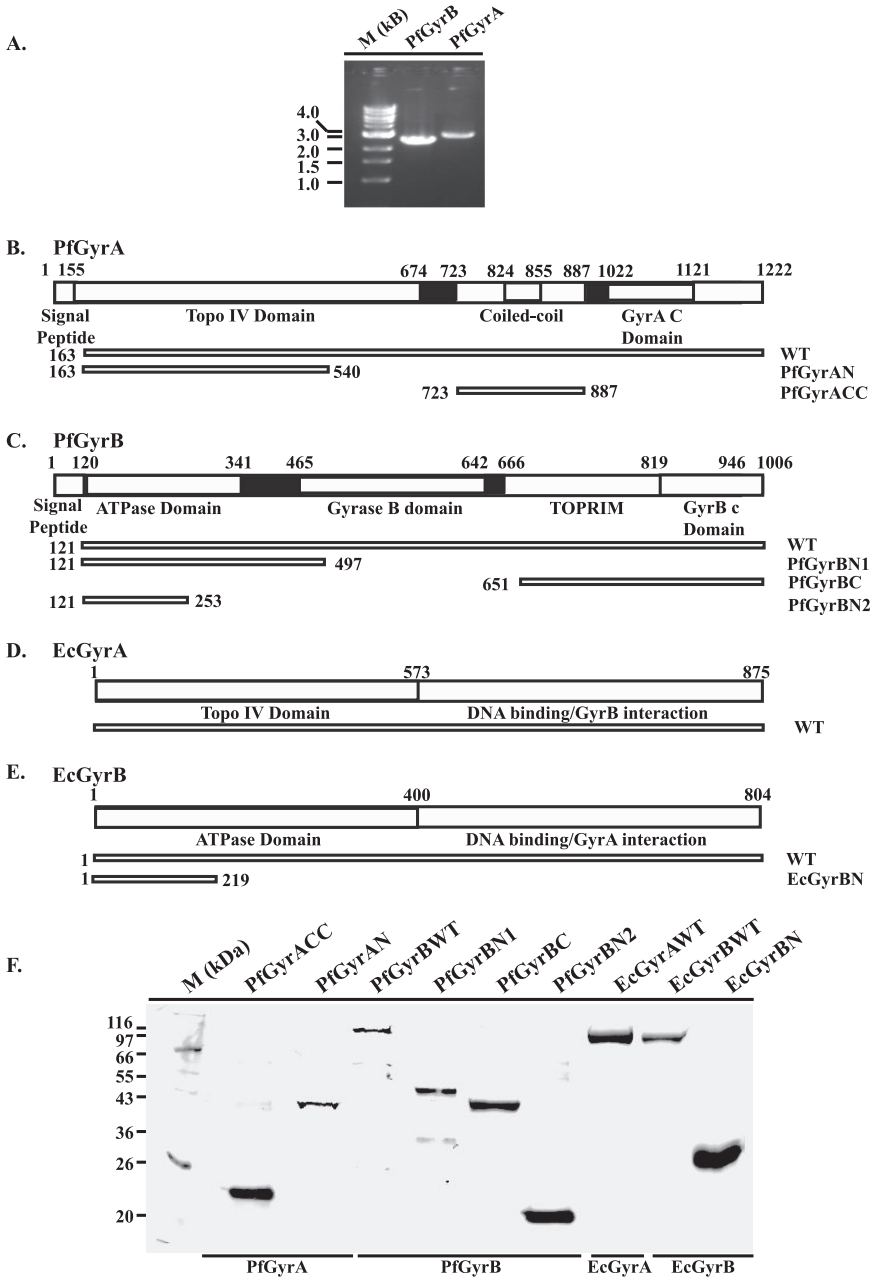


FIG. 1. Cloning, expression, and purification of full-length and different deletion mutants of Pf*gyrA*/*B* and Ec*gyrA*/*B* genes. (A) PCR amplification of Pf*gyrA* and Pf*gyrB* genes. The lanes from left to right show the DNA ladder and amplified Pf*gyrB* and Pf*gyrA* gene products, respectively. (B to E) Schematic representation of PfGyrA, PfGyrB, EcGyrA, and EcGyrB polypeptides showing the putative functional domains. The dark patches inside the main blocs represent low-complexity regions. The wild type and different deletion mutants of each polypeptide used in this study are also shown along with their respective amino acid positions. (F) Purification of the wild type and deletion mutants of PfGyr/EcGyr A and B subunits. Different proteins, as indicated at the top, were purified using Ni-nitrilotriacetic acid affinity purification and subjected to 10% SDS-PAGE followed by Coomassie staining as described in Materials and Methods. "M" indicates molecular mass markers (in kilodaltons).

and purify two functional domains of PfGyrA (PfGyrAN and PfGyrACC).

**Expression of PfGyrA and PfGyrB at the transcript and protein levels.** In order to find out whether PfGyrA and PfGyrB are truly expressed at the mRNA level during the asexual erythrocytic stages, RT-PCR analysis was performed using cDNA isolated from various erythrocytic stages. Total RNA was extracted from ring-, trophozoite-, and schizont-stage parasites, which was followed by the preparation of cDNA according to protocols described in Materials and Methods.

Analysis of the RT-PCR product revealed that PfGyrA is expressed mostly during the trophozoite and schizont stages (Fig. 2A). The expression of PfGyrB could be detected during the ring stage, although the expression level peaked during later stages. In order to rule out the possibility of genomic DNA contamination in the cDNA, total RNA was treated with

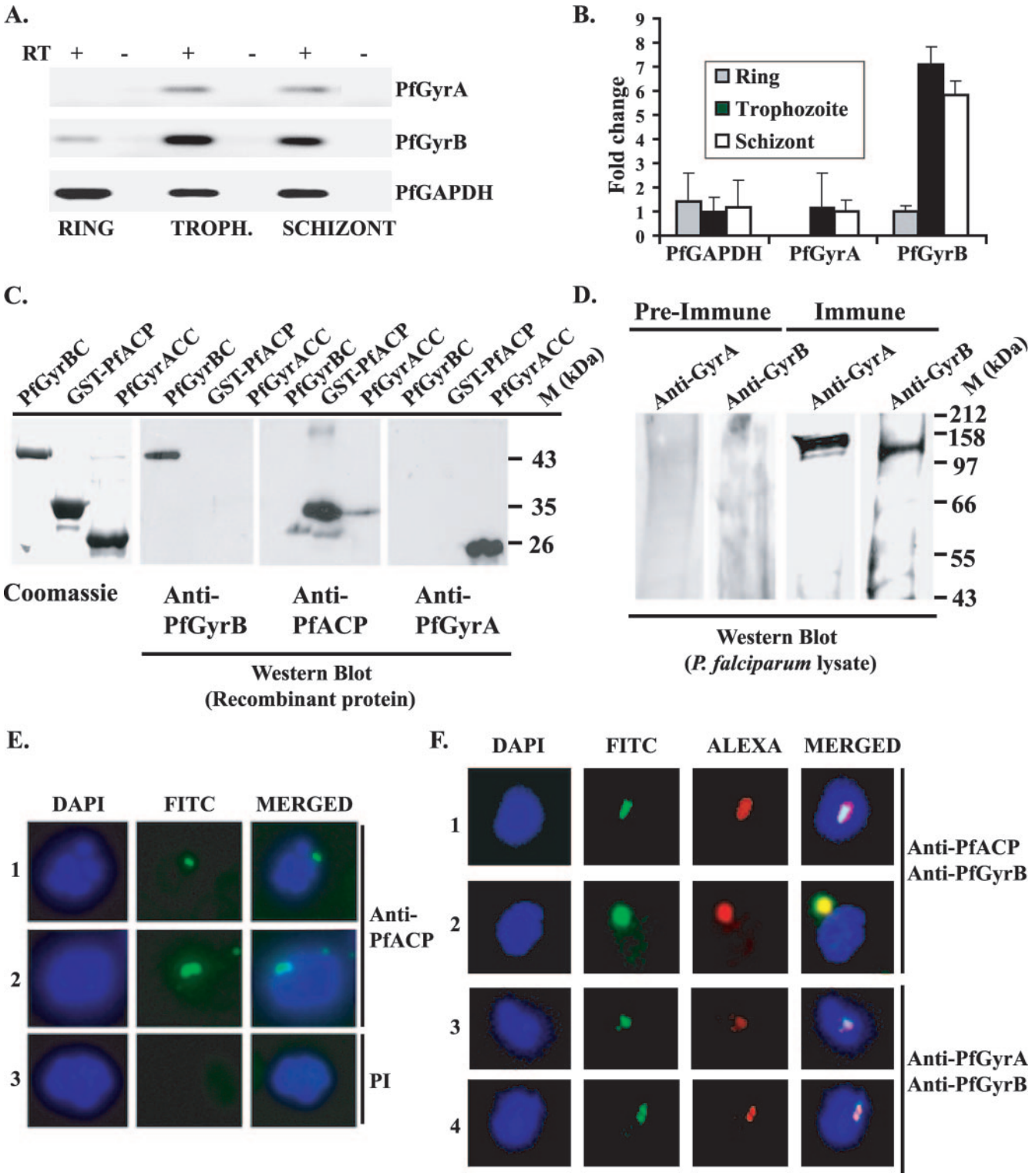


FIG. 2. Stage-specific expression and apicoplast localization of PfGyrA/B. (A) RT-PCR analysis of PfGyrA and PfGyrB. RT-PCR products of PfGyrA, PfGyrB, and PfGAPDH were obtained by using the cDNA templates from ring, trophozoite (TROPH.), and schizont stages of the parasite life cycle and electrophoresed in a 1% agarose gel. RT lanes with a + indicate PCR products that were obtained by using a cDNA template, and RT lanes with a − indicate the negative control. GAPDH was used as the loading control. (B) Changes (*n*-fold) in the expression of PfGyrA, PfGyrB, and PfGAPDH at the mRNA level at different erythrocytic stages of the parasites. The relative intensity of each band was calculated using densitometry scanning, and the absolute values were obtained by normalizing them against the background intensity. This figure shows the averages of three independent sets of different experiments. (C) Specificities of anti-PfGyrB, anti-PfACP, and anti-PfGyrA antibodies. The Coomassie-stained SDS-PAGE gel in the left panel shows purified $His_6$-PfGyrBC, GST-PfACP, and $His_6$-PfGyrACC, which were used as immunogens to raise the antibodies in animals. In the Western blot analysis (right three panels), the respective antibodies recognized the antigens

DNase I, and it was processed similarly to how it was done for cDNA preparation, except for the addition of reverse transcriptase enzyme (Fig. 2A). No products were obtained in these lanes, suggesting that RT products were not contaminated with genomic DNA. As an internal control, a specific region of Pf*GAPDH* was amplified using specific primers shown in Table S2 in the supplemental material. The RT-PCR analysis was repeated three times. For quantitation, the relative intensity of each band from each experiment was calculated by densitometry scanning, and absolute values were obtained by normalizing against the background intensity (34). After careful analysis of these results, it was found that the expression level of control glyceraldehyde-3-phosphate dehydrogenase (GAPDH) fluctuates between 1 and 1.7 during the different erythrocytic stages. The expression level of PfGyrB peaks at the trophozoite stage, with a slight decrease in the schizont stage. On an absolute scale, these values increased six to eight times at the later stages compared to that of the ring stage (Fig. 2B). The expression level of PfGyrA was low compared to those of PfGyrB and GAPDH. PfGyrA expression could be detected only during the trophozoite and schizont stages. It is interesting that apicoplast DNA replication overlaps with nuclear DNA replication (5, 28, 38, 56). Since nuclear DNA replication takes place during the late trophozoite and schizont stages (24), it can be suggested that the expression patterns of PfGyrA and PfGyrB coincide with the time of DNA replication.

In order to investigate the expression of PfGyrA and PfGyrB at the protein level, specific antibodies were raised against purified antigens as shown in Fig. 2C. Anti-PfGyrA antibodies were raised in mice, whereas anti-PfGyrB antibodies were raised in rabbits. It has been shown previously that ACP is an apicoplast-targeted protein (39, 52). ACP was purified as a GST fusion protein, and polyclonal antibodies were raised against the purified antigens in mice. To check the specificities of these antibodies, Western blot analysis was performed as shown in Fig. 2C. It was found that these antibodies could specifically detect only the antigens against which they were generated without showing any cross-reactivity with other antigens (Fig. 2C). Other anti-PfGyrA and anti-PfGyrB antisera were used for Western blot analysis using parasite lysates obtained from late trophozoite/early schizont stages. The theoretical molecular masses of PfGyrA and PfGyrB are ~143 kDa and ~116 kDa, respectively. Both antibodies recognized predominantly a single band close to their deduced molecular masses (Fig. 2D). Preimmune sera under the same experimental conditions failed to recognize any such band, suggesting that these proteins are truly expressed in the parasites.

Analysis of the amino-terminal sequences of both PfGyrA and PfGyrB suggests the presence of an apicoplast-targeting sequence comprising the transit peptide as well as the signal peptide. In order to find out whether these proteins are truly localized in the apicoplast, immunofluorescence experiments were performed. Glass slides containing thin smears of the parasites from different stages (as indicated in the figure legends) were prepared, and they were processed for the immunofluorescence experiments. Initially, to determine the specific location of the apicoplast, we performed immunofluorescence assays using anti-GST-PfACP antibodies as a positive control. We found a strong subnuclear green signal characteristic of the apicoplast (Fig. 2E, panels 1 and 2). Preimmune sera under the same experimental conditions did not show any signal (Fig. 2E, panel 3). Following confirmation of the apicoplast localization of PfACP, we performed colocalization experiments using a mixture of anti-PfGyrB and anti-PfGyrA or anti-GST-PfACP antibodies as described in Materials and Methods. Fluorescein isothiocyanate-conjugated and Alexa red (Santa Cruz) secondary antibodies were used in these cases, and the green or red fluorescence was monitored by using a NIKON fluorescence microscope. Several hundred cells were scanned for cellular localization as shown in Fig. 2E and F. The green fluorescence and red fluorescence were detected in a subnuclear compartment, and they merged reasonably well with each other (Fig. 2F). In the upper two panels of Fig. 2F, the signals of the apicoplast-targeted protein ACP and PfGyrB overlapped with each other, and in the lower two panels, PfGyrA and PfGyrB signals merged with each other. Since ACP has previously been shown to be specifically located at the apicoplast, these results together suggest that PfGyrA and PfGyrB are localized in the apicoplast. Preimmune sera under the same experimental conditions do not show any signal that further confirms the specificity of these antibodies (data not shown).

***P. falciparum gyrB* complements an *E. coli* temperature-sensitive strain.** To further determine whether these putative Pf*gyr* genes code for functional gyrase proteins, functional genetic complementation in *E. coli* was performed (51). For this purpose, *E. coli gyrA* temperature-sensitive mutant cells were transformed with pAD1 containing the Pf*gyrA* gene, and *E. coli gyrB* temperature-sensitive mutant cells were transformed with pAD2 containing the Pf*gyrB* gene. pAD1 and pAD2 are the derivatives of pHH3 and pAG111 containing Ec*gyrA* and

against which they were raised without cross-reaction with other antigens. "M" indicates the molecular mass ladder. (D) 3D7 parasite pellets enriched in late trophozoite/early schizont stages were boiled in SDS-PAGE loading buffer, and the supernatant was treated for SDS-PAGE analysis followed by Western blot analysis using either anti-PfGyrA or anti-PfGyrB antibody (1:500 dilution) or the corresponding preimmune sera. Molecular mass markers are shown on the right. (E) Localization of PfACP in the apicoplast. An immunofluorescence assay was performed using anti-PfACP primary antibodies and fluorescein isothiocyanate (FITC)-conjugated secondary antibodies on glass slides containing thin smears of nonsynchronized *P. falciparum* parasites as described in Materials and Methods. Panels 1 and 2 show that PfACP (green) is localized to the apicoplast. No signal was obtained in panels where control preimmune serum was used. DAPI (4′,6′-diamidino-2-phenylindole) was used to stain the nuclei. (F) Apicoplast localization of PfGyrA and PfGyrB. An immunofluorescence assay was performed using the above-described antibodies on glass slides containing thin smears of *P. falciparum* parasites (mostly late trophozoite stages) as described in Materials and Methods. In panels 1and 2, PfACP (green) and PfGyrB (red) are colocalized to the apicoplast. In the third and fourth panels, PfGyrA (green) and PfGyrB (red) show colocalization to the apicoplast. PfGyrB was probed with anti-PfGyrB antibody (rabbit, 1:500 dilutions), PfACP was probed with anti-PfACP antibody (mouse, 1:1,000 dilutions), and PfGyrA was probed with anti-PfGyrA antibody (mouse, 1:500 dilution). In all cases, nuclei were counterstained with DAPI.

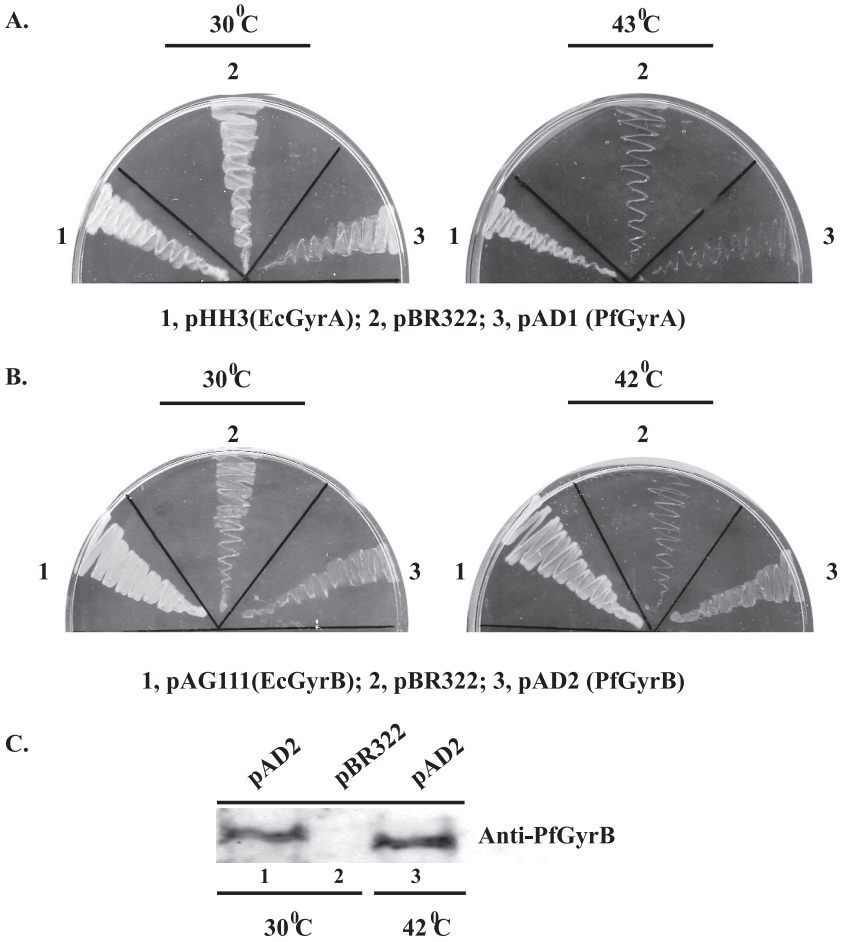


FIG. 3. Complementation analysis of *E. coli* temperature-sensitive strains KNK453 and N4177 with plasmids pAD1 and pAD2 carrying Pf*gyrA* and Pf*gyrB* genes. (A) *E. coli* strain KNK453 was transformed with (i) pHH3, (ii) pBR322, or (iii) pAD1 containing Pf*gyrA*. Bacterial cells were plated onto LB agar plates and incubated at either a permissive temperature (30°C) or a nonpermissive temperature (43°C). (B) *E. coli* strain N4177 was transformed with either (i) pAG111, (ii) pBR322, or (iii) pAD2 containing Pf*gyrB*. Transformed bacteria were incubated at a permissive temperature (30°C) or a nonpermissive temperature (42°C). (C) Detection of expression of PfGyrB in N4177 cells by immunoblotting using anti-PfGyrB antibody. Lanes 1 and 3 contained extract from pAD2-transformed N4177 cells at permissive (30°C) and nonpermissive (42°C) temperatures, while lane 2 contained extracts from the pBR322-transformed N4177 cells at a permissive (30°C) temperature.

Ec*gyrB* genes, respectively (26). We found that Pf*gyrA* failed to complement *E. coli* temperature-sensitive cells at the restrictive temperature, whereas PfGyrB could do that nicely at the restrictive temperature (Fig. 3A and B, respectively). *E. coli gyrA* and *gyrB* genes could rescue these temperature-sensitive phenomena at the restrictive temperature nicely, whereas the control, pBR322, could not rescue these phenotypes under the same experimental conditions. Pf*gyrA* was not expressed in the mutant *E. coli* strain even at 30°C (nonrestrictive temperature), as anti-Pf*gyrA* antibodies failed to detect any band following Western blot analysis of the lysate obtained from Pf*gyrA*-transformed *E. coli* cells (data not shown). However, Pf*gyrB* was expressed nicely in the *E. coli gyrB* mutant cells at both the normal temperature and the restrictive temperature following Western blot analysis, as shown in Fig. 3C. These results suggest that Pf*gyrB* is a true *gyrB* homologue.

**Analysis of intrinsic ATPase activity of PfGyrB (WT) and other deletion mutants.** In order to assess the ATPase activity of PfGyrB and its stimulation in the presence of DNA or a GyrA subunit, we performed an ATPase assay using either wild-type or different deletion mutants of PfGyrB. We found that full-length PfGyrB showed the maximum activity, followed by PfGyrBN1, whereas PfGyrBN2 and PfGyrBC did not show any activity (Fig. 4A). The ATPase domain of gyrase B is confined to the N terminus domain that is included in the deletion mutant N1. This result is similar to the recently published report on the N-terminal ATPase domain of the *P. vivax* GyrB subunit, which also shows in vitro ATPase activity (30). These experiments also suggest that unlike EcGyrB, PfGyrB shows strong intrinsic ATPase activity. In order to determine whether the intrinsic ATPase activity of PfGyrB is not due to the presence of any contaminant in the protein preparation, we made a single point mutation at the conserved glutamic acid (E159 to A) residue within the ATPase domain. The mutation in the equivalent glutamic acid residue (E42) in EcGyrB completely eliminates the ATPase activity (29). The mutant protein did not show any ATPase activity compared with the wild

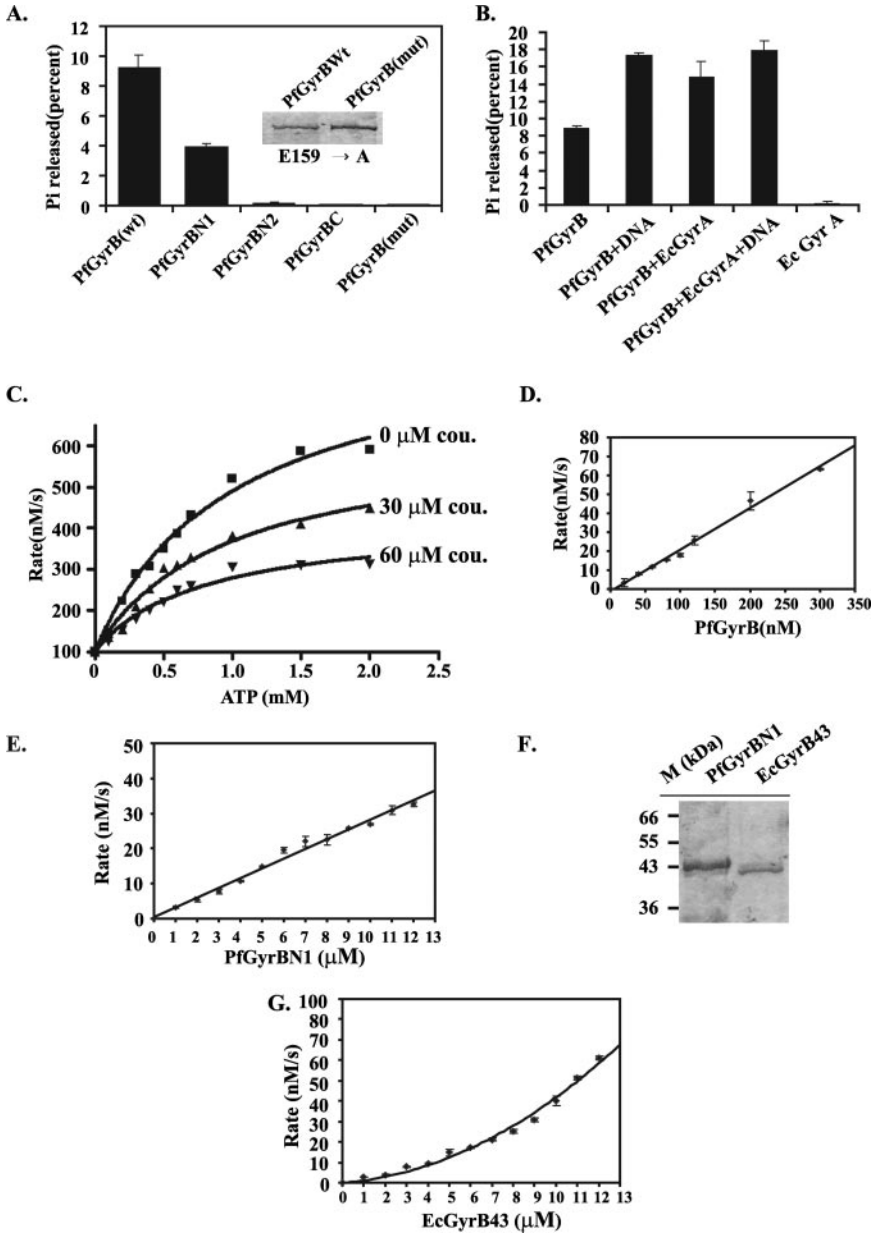


FIG. 4. ATPase activity of *P. falciparum* gyrase B. In the cases of A and B, an ATPase assay was carried out in supercoiling buffer in the presence of 1 mM cold ATP and 3.4 fmol [$\gamma$-$^{32}$P]ATP, while in the cases of C, D, E, and G, the reactions were carried out by an NADH-coupled enzymatic reaction (as described in Materials and Methods). (A) Comparison of the intrinsic ATPase activities of PfGyrB (WT), different deletion mutants (as indicated), and a PfGyrB mutant [PfGyrB(mut)] with a point mutation as indicated in the inset, which shows the purification of wild-type and mutant proteins. All the proteins were simultaneously purified and added to the reaction mixture in equimolar amounts (90 nM). ATPase activity could be detected only in PfGyrB (WT) and PfGyrBN1. (B) Stimulation of the intrinsic ATPase activity of PfGyrB with EcGyrA and DNA. The reactions were carried out in the presence of 90 nM PfGyrB (WT) and/or 90 nM EcGyrA and/or 10 μg/ml linear pBR322 DNA wherever applicable. (C) Effect of coumermycin on the ATPase activity of PfGyrB. Various concentrations of the drug coumermycin A1 (cou.) (0, 30, and 60 μM) (as indicated in the figure with "■," "▲," and "▼" symbols, respectively) were added at different substrate (ATP) concentrations in the reaction mixture containing 200 nM PfGyrB enzyme, and ATP hydrolysis rates were measured. (D) Linear rate of ATP hydrolysis by PfGyrB (WT) with ATP at a concentration of 2 mM and various amounts of enzymes. (E) Rate of ATP hydrolysis of PfGyrBN1 (~43 kDa) with ATP at a concentration of 2 mM with increasing amounts of enzymes. (F) Purification and Coomassie staining of PfGyrBN1 (PfGyrB43) and EcGyrB43 proteins. (G) Nonlinear rate of ATP hydrolysis of EcGyrB43 under the same experimental conditions as those for E. Each experiment was repeated at least three times, and the results are quantitated and plotted graphically with error bars.

type, further confirming that the intrinsic ATPase activity of PfGyrB is real (Fig. 4A).

One of the hallmarks of EcGyrB ATPase activity is its stimulation in the presence of DNA and EcGyrA (33, 50). We found that the addition of DNA or EcGyrA alone can stimulate the ATPase activity of PfGyrB to almost twice that of PfGyrB alone (Fig. 4B). The addition of both DNA and EcGyrA does not stimulate the ATPase activity significantly

compared to those of EcGyrA or DNA addition lanes (Fig. 4B). EcGyrA does not show any activity, suggesting that PfGyrB is able to form an active complex with an EcGyrA counterpart that leads to the stimulation of ATPase activity. These results together suggest that PfGyrB shows intrinsic ATPase activity that can be stimulated in the presence of DNA or GyrA.

Coumermycin is a potent selective drug for bacterial gyrases (50). In order to test the effect of this drug on PfGyrB (WT), ATP hydrolysis rates were measured in the absence and presence of various drug concentrations. We found that increasing concentrations of coumermycin could inhibit the rate of ATP hydrolysis of PfGyrB in a dose-dependent manner (Fig. 4C). In the absence of drug, PfGyrB (WT) ATPase activity shows typical hyperbolic dependence on substrate concentration, with a $K_m$ value of 1.05 mM (Fig. 4C; see Fig. S2 in the supplemental material) that is comparable to the $K_m$ value observed for the 43-kDa domain of *E. coli* GyrB (0.68 mM) (1). The addition of coumermycin inhibited PfGyrB (WT) enzyme-catalyzed ATP hydrolysis with a $K_i$ value of ~40 μM (see Fig. S2 in the supplemental material). This value is ~500 times higher than the $K_i$ of EcGyrB (~80 nM) (48) and ~28-fold higher than the $K_i$ value of the 45-kDa *P. vivax* GyrB ATPase domain (1.4 μM) (30).

The rate of ATP hydrolysis with increasing full-length PfGyrB (WT) enzyme concentrations was monitored (Fig. 4D). The ATP hydrolysis rate was found to be linear with increasing enzyme concentrations under our experimental conditions. However, due to the low yield of PfGyrB (WT) enzyme, the ATP hydrolysis rate could not be monitored at higher enzyme concentrations. In order to circumvent this problem, the ATP hydrolysis rate was calculated using increasing amounts of PfGyrBN1 (~43 kDa) (Fig. 4E), which gave us better yields and showed ATPase activity (Fig. 4A). The ATP hydrolysis rates of PfGyrBN1 (Fig. 4E) and the equivalent protein EcGyrB43 (Fig. 4G) were compared (purification of both the proteins is shown in Fig. 4F). It was reported previously that EcGyrB43 shows a nonlinear pattern of ATP hydrolysis (1). We observed that PfGyrBN1 followed a linear pattern of ATP hydrolysis with increasing amounts of enzyme even at higher enzyme concentrations under our experimental conditions (Fig. 4E). Interestingly, the equivalent protein EcGyrB43 followed a nonlinear pattern under the same experimental conditions, as reported previously (Fig. 4G). Therefore, we conclude that unlike EcGyrB, PfGyrB shows a linear pattern of ATP hydrolysis.

**DNA cleavage and DNA supercoiling activity of PfGyrB in combination with EcGyrA or PfGyrAN.** The GyrA protein is involved in the DNA breakage and reunion aspects of the supercoiling reaction, whereas the GyrB protein is responsible for ATP hydrolysis. The essential step in the DNA supercoiling pathway is the cleavage of DNA in both strands. Ciprofloxacin, a member of the quinolone family of drugs, interrupts the cleavage and rejoining of the DNA strands. The addition of SDS in such a trimeric reaction containing DNA, gyrase, and drugs and the subsequent digestion of the protein lead to the appearance of cleaved DNA. It has also been shown that the addition of $CaCl_2$ instead of $MgCl_2$ in the gyrase reaction mixture leads to a double-stranded DNA break at the same site as those created by quinolone drugs. The N terminus of EcGyrA, together with full-length EcGyrB, is sufficient to perform the DNA cleavage of supercoiled DNA (41).

We were interested to see whether the combination of PfGyrAN and PfGyrB (WT) could lead to a functional complex that can perform DNA cleavage and a supercoiling reaction. For this purpose, we first performed a $Ca^{2+}$-directed DNA cleavage reaction followed by the separation of these products in an agarose gel, as described in Materials and Methods, by using various combinations of *E. coli* and *P. falciparum* gyrase enzymes. We found that PfGyrAN together with PfGyrB could efficiently cleave supercoiled DNA that could be stabilized by the use of $Ca^{2+}$ (Fig. 5A, lanes 4 and 5). The combination of *E. coli* and *P. falciparum* gyrase subunits also stimulates the DNA cleavage reaction in a $Ca^{2+}$-dependent manner (Fig. 5A, lanes 2 and 3), compared to the control lane (lane 1). It was also found that an active complex of PfGyrA and PfGyrB is required for this reaction, since neither PfGyrA nor PfGyrB alone could perform these reactions (Fig. 5A, lanes 6 and 7). The intensities of the linear cleaved products (Fig. 5A) were quantified using densitometry scanning, and the relative DNA cleavage activities were plotted as shown in Fig. 5B.

It was shown previously that topoisomerase II inhibitors can induce the cleavage of nuclear and apicoplast DNA in *P. falciparum* (55). To investigate whether a recombinant PfGyr complex can perform a DNA cleavage reaction in the presence ciprofloxacin, a series of experiments was performed in the absence or presence of increasing amounts of ciprofloxacin using either the *E. coli* or the *P. falciparum* gyrase enzyme complex. The results shown in Fig. 5C indicate that both the EcGyr and PfGyr complexes show DNA cleavage activity in the presence of ciprofloxacin. Furthermore, PfGyr shows this activity in a dose-dependent manner (Fig 5C, lanes 4 to 8). The addition of EDTA in the reaction mixture following incubation of the PfGyr complex in the presence of DNA and ciprofloxacin resulted in the reversion of the DNA cleavage reaction (Fig. 5C, lane 9), suggesting that the cleavage reaction is truly performed by the PfGyr complex. Ciprofloxacin-mediated relative DNA cleavage activities are plotted in Fig. 5D. Together, these results (Fig. 5A to D) suggest that PfGyrAN and PfGyrB (WT) enzymes are functionally active.

Furthermore, to show whether the complex formed between these two *Plasmodium* enzymes could perform a supercoiling reaction, we checked their activities on relaxed DNA using several combinations of *E. coli* and *Plasmodium* enzymes in the presence of ATP. We observed that the gyrase complex comprising *E. coli* A and B subunits could transform relaxed DNA into supercoiled DNA nicely, suggesting that our reaction conditions are optimal for the supercoiling assay (Fig. 5E). PfGyrB together with EcGyrA could also transform relaxed DNA into supercoiled DNA in a dose-dependent manner to a very limited extent, suggesting that the ATPase activity of PfGyrB could be used for the supercoiling reaction in combination with EcGyrA in vitro (7, 46). The relatively poor activity of EcGyrA and PfGyrB complexes in the supercoiling reaction could be due to the fact that supercoiling is thermodynamically unfavorable compared to other gyrase activities. The addition of PfGyrAN in a reaction mixture containing PfGyrB did not lead to the supercoiling of relaxed DNA (Fig. 5E), suggesting that although PfGyrAN contained efficient DNA cleavage activity, it might not retain all the functions required for DNA super-

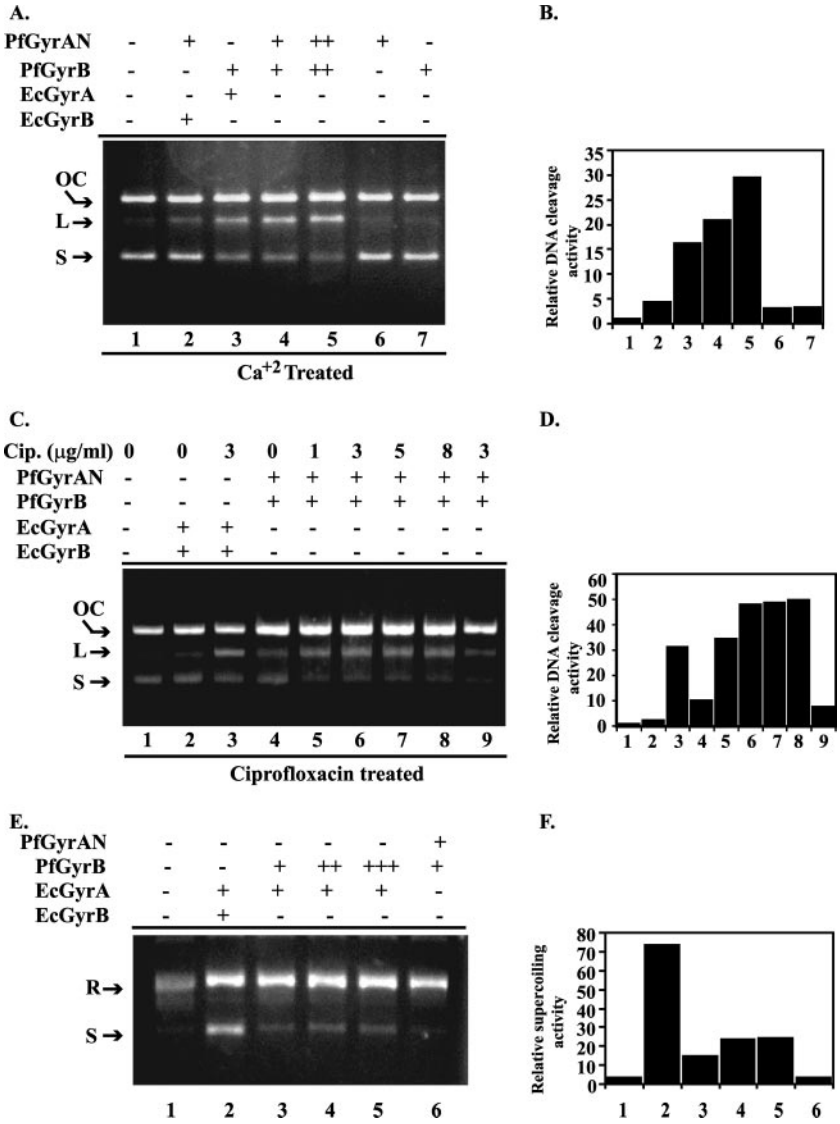


FIG. 5. DNA cleavage and supercoiling activity of *P. falciparum* gyrase. (A) $CaCl_2$-induced DNA cleavage. Ten micrograms of supercoiled pBR322 DNA per milliliter was incubated with 70 nM each PfGyrAN and EcGyrB (lane 2), 70 nM each EcGyrA and PfGyrB (lane 3), 70 nM each PfGyrAN and PfGyrB (lane 4), 100 nM each PfGyrAN and PfGyrB (lane 5), 70 nM PfGyrAN alone (lane 6), or 70 nM PfGyrB alone (lane 7) in a total reaction mixture volume of 30 μl. Lane 1 does not contain any protein. The experimental procedure is discussed in Materials and Methods. + and − indicate the presence or absence, respectively, of a particular protein in that reaction mixture. OC, open circular form of DNA; L, linear form of DNA; S, supercoiled form of DNA. (B) Intensities of the linear bands following $CaCl_2$-induced DNA cleavage reactions were quantitated by densitometry scanning, and the values were plotted graphically. (C) Ciprofloxacin-induced DNA cleavage. The EcGyr or PfGyr complex (70 nM each protein) was incubated for 1 h in the absence (lanes 2 and 4) or presence (lanes 3 and 5 to 8) of different concentrations of ciprofloxacin (Cip.) (as indicated at the top), followed by SDS and proteinase K treatment and agarose gel electrophoresis of the reaction products as discussed in Materials and Methods. Lane 1 did not contain any protein, and in lane 9, 10 mM EDTA was added before the addition of SDS and proteinase K to show the reversibility of DNA cleavage reaction. (D) Intensities of the linear bands following ciprofloxacin-induced DNA cleavage reactions were quantitated, and the values were plotted to obtain the relative DNA cleavage activity. (E) Supercoiling reaction of PfGyrB in combination with EcGyrA and PfGyrAN. Ten micrograms of relaxed pBR322 DNA per milliliter was incubated in supercoiling buffer (see Materials and Methods) with 70 nM EcGyrA in combination with 70 nM EcGyrB (lane2), 70 nM PfGyrB (lane3), 100 nM PfGyrB (lane 4), or 130 nM PfGyrB (lane5). Lane 6 contains 100 nM each of PfGyrAN and PfGyrB. (F) The intensities of supercoiled DNA bands were quantified and are represented by bar graphs.

coiling activity. These results are also represented graphically in Fig. 5F. In a control reaction, none of the gyrase subunits alone can perform the supercoiling activity by themselves (data not shown), suggesting that the combination of active gyrase A and B subunits is required for supercoiling activity.

**Dimerization of PfGyrB and PfGyrA subunits.** The intrinsic ATPase activity of PfGyrB and its linear rate of ATP hydrolysis suggest that there are some differences in PfGyrB compared to its *E. coli* counterpart. It was previously shown that *E. coli* GyrB forms a dimer in the presence of a nonhydrolyzable

analogue of ATP (ADPNP) or competitive inhibitors of ATP hydrolysis (coumermycin) that can account for the nonlinear rate of ATP hydrolysis of this enzyme (1, 23, 47). We wanted to verify whether this was true for PfGyrB. For this purpose, we purified the N-terminal minimal region of PfGyrB (as shown in Fig. 6A) and the equivalent counterpart, EcGyrB (containing the conserved Ile128 residue that has been shown to be essential for the dimerization of EcGyrB). Glutaraldehyde cross-linking experiments were performed in order to detect the dimer forms of these proteins in the absence and presence of coumermycin. We found that PfGyrBN2 could form strong and stable dimers in the absence of the drug, as shown by glutaraldehyde cross-linking followed by Western blot analysis with anti-$His_6$ antibodies (Fig. 6B). On the contrary, only a fraction of the EcGyrBN formed dimers in the presence of the drug only. These results confirm the ATP-dependent dimerization of EcGyrB as reported previously and also suggest that the interfaces required for the ATP-independent dimerization of PfGyrBN2 might be different.

To prove that the dimerization of $His_6$-PfGyrBN2 is not due to the addition of a $His_6$ fusion tag, cross-linking experiments using maltose binding protein (MBP)-tagged PfGyrBN2 in the absence of ATP analogues were performed. Following Western blot analysis using anti-MBP antibodies, cross-linked products (~128 kDa) were obtained in the presence glutaraldehyde for MBP-PfGyrBN2 only (Fig. 6C, lanes 1 and 2). MBP alone did not yield any cross-linked product under the same experimental conditions (Fig. 6C, lanes 3 and 4), suggesting that the dimerization event is not the outcome of the inclusion of a fusion tag. Finally, in order to evaluate the efficacy of dimer formation of full-length PfGyrB (wild type) (~103 kDa), cross-linking experiments were performed using full-length $His_6$-PfGyrB (Fig. 6D). Western blot analysis using anti-His-tagged polyclonal antibodies revealed dimer formation (~206 kDa) in the presence of glutaraldehyde and in the absence of ATP. These results suggest that full-length PfGyrB has the potential to form dimers in the absence of ATP analogues like PfGyrBN2.

In *E. coli*, the mutation of an isoleucine residue equivalent to Ile128 in PfGyrB completely abrogates the ATP-dependent dimerization (6). To test whether Ile128 plays a similar role in the dimerization of PfGyrB, a point mutation was made in PfGyrBN2 (Ile128 to Gly), and the mutant protein was subjected to glutaraldehyde cross-linking followed by Western blot analysis using anti-His antibodies (Fig. 6E and F). To our surprise, the mutation in the Ile128 residue alone did not affect dimer formation. These results suggest that residues other than the Ile128 are important for the ATP-independent dimerization of PfGyrB. Further detailed experiments are required to find out the exact residues or region in PfGyrB that might account for the dimer formation.

In order to rule out any possibility that the results of the cross-linking experiments were due to technical artifacts, PfGyrBN2 and PfGyrBN2M were subjected to native PAGE analysis where both the proteins comigrated along with the control, ovalbumin (~43 kDa) (Fig. 6G). In the SDS-PAGE analysis, $His_6$-PfGyrBN2 showed an apparent molecular mass of ~22 kDa, which is very close to the molecular mass deduced from the amino acid sequence (~19 kDa) (Fig. 1F and 6B). Therefore, the results obtained from native PAGE analysis strongly suggest that PfGyrB forms a stable dimer in solution in the absence of ATP and rule out any possibility of technical artifacts in the cross-linking experiments.

Finally, we performed gel filtration chromatography using either wild-type PfGyrB, PfGyrBN1, or PfGyrBN2 in the absence of ATP. These proteins were subjected to size-exclusion chromatography using a Superose-12 gel filtration column, which can be used to separate a broad range of proteins. The column was first calibrated using different high- and low-molecular-mass gel filtration standards. Figure 6H shows the elution patterns of these standard proteins. Following calibration, all the proteins (500 μg each) described above were subjected to chromatographic separation under the same experimental conditions in the absence of ATP. Fractions were collected (0.5 ml each) and further analyzed by SDS-PAGE. The elution patterns of these proteins are shown in Fig. 6H. The peak fraction of wild-type PfGyrB (~103 kDa) overlapped with the peak fraction of a standard catalase that has a molecular mass of ~232 kDa, suggesting that wild-type PfGyrB is a dimer in solution, as suggested by cross-linking experiments (Fig. 6D). The peak fraction of PfGyrBN1 (~43 kDa) eluted in fraction 29. The BSA standard eluted in fraction 30. These results suggest that PfGyrBN1 in solution is possibly a dimer. The elution pattern of PfGyBN2 (~22 kDa) was little different. One peak was observed around fraction 18. We think these are multimeric forms of PfGyrBN2 or aggregation products of a monomeric protein. However, there was another peak at fraction 32 that coincides with the molecular mass standard of 43 kDa. We believe that these are dimeric forms of PfGyrB, as suggested by the cross-linking experiments (Fig. 6A). Presently, we do not know the exact biophysical properties of the high-molecular-weight fractions of PfGyrBN2. However, it is clear that they will not enter the gel following cross-linking. Very little protein coeluted in fraction 36, which is supposed to be the position of the monomeric PfGyrBN2 (~22 kDa) protein. These experiments together suggest that PfGyrB is mostly a dimer in solution. Furthermore, the molecular masses of these proteins were also deduced by plotting the log molecular mass of the standards against the fraction numbers (see Fig. S3 in the supplemental material). The standard curve thus obtained helped to deduce the apparent molecular masses of all three proteins (as eluted by gel filtration chromatography), which were very close to double the molecular mass of each protein (PfGyrB [WT], ~199.5 kDa; PfGyrBN1, ~97.7 kDa; PfGyrBN2, ~39.8 kDa).

*E. coli* gyrase forms a heterotetrameric complex, $A_2B_2$, comprised of A and B subunits. However, each A and B subunit forms dimers. It was previously shown that residues 363 to 494 are important for the dimerization of EcGyrA (13, 14). This region does not show any homology with PfGyrA. However, upon careful analysis of the PfGyrA sequence, we found a unique leucine heptad repeat at the C terminus between residues 835 and 856 (Fig. 6I). This region also shows a coiled-coil domain as predicted by PAIRCOIL software. The BZIP type of leucine zipper is often found in several transcription factors, including jun and fos, that form dimers followed by DNA binding (60). We were tempted to test whether this region in PfGyrA forms a dimer. To test this, we purified $His_6$-PfGyrCC containing the leucine heptad repeat and performed glutaraldehyde cross-linking followed by Western blot analysis using

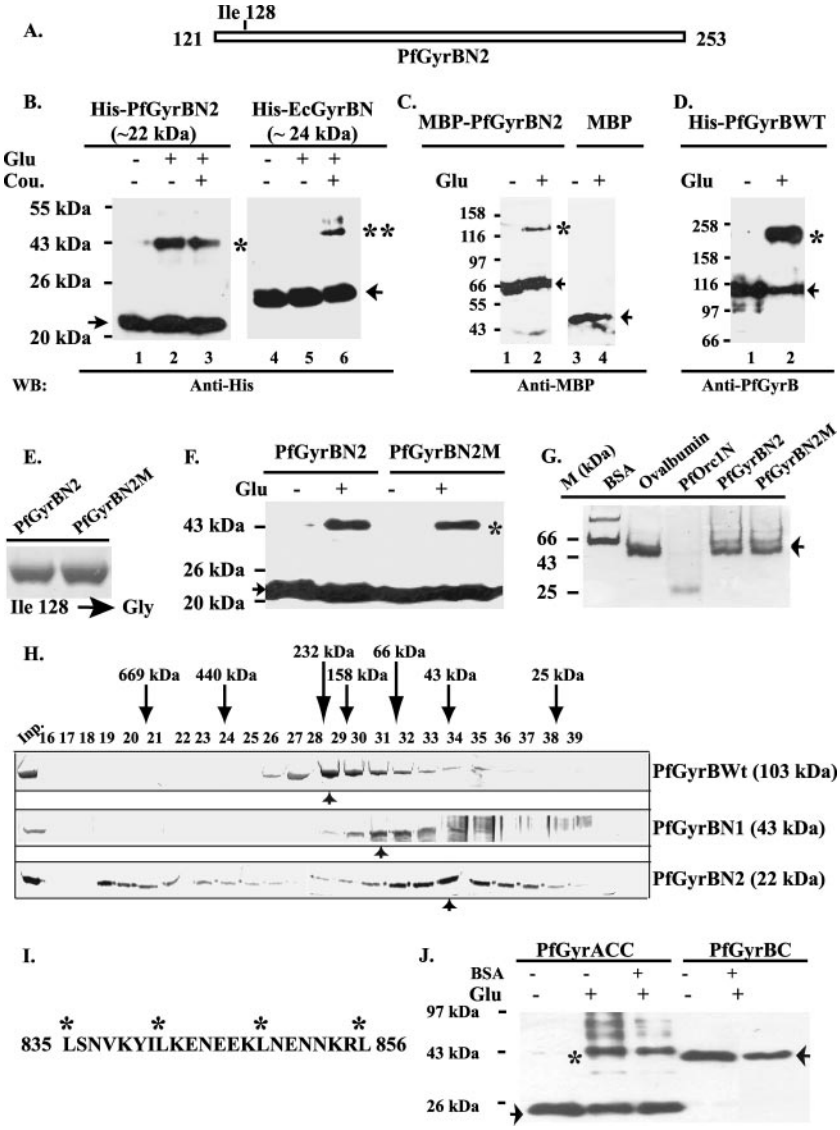


FIG. 6. PfGyrB and PfGyrA are homodimers in solution. (A) Schematic diagram of the PfGyrBN2 ATPase domain containing the dimerization interface. The conserved residue Ile128 is marked. (B) Comparison of the glutaraldehyde cross-linking products of PfGyrBN2 and EcGyrBN (1.0 μM each) in the presence or absence of the drug coumermycin (Cou.) (0.5 μM). "*" and "**" indicate the positions of the dimerized products for PfGyrBN2 and EcGyrBN, respectively. (C) Glutaraldehyde cross-linking of MBP-tagged PfGyrBN2 (~64 kDa) (lanes 1and 2) or MBP alone (lanes 3 and 4). Experiments were carried out as described above (B), except for the Western blot analysis using anti-MBP polyclonal antibodies and without the addition of ATP analogues. Arrows indicate the positions of the monomer, and the asterisk (*) indicates the position of the dimer (~128 kDa). (D) Cross-linking of $His_6$-tagged full-length P*fgyrB* in the absence or presence of glutaraldehyde (lanes 1 and 2, respectively). The arrow indicates the position of the monomer (~103 kDa), and the asterisk (*) indicates the position of the dimer (~206 kDa). (E) Purification of PfGyrBN2 and PfGyrBN2M with a point mutation at Ile128. (F) Glutaraldehyde cross-linking status of the above-mentioned proteins. (G) Native PAGE analysis of PfGyrBN2 and PfGyrBN2M. One microgram of each protein was loaded onto a 10% polyacrylamide native gel followed by Coomassie staining. BSA (66 kDa), ovalbumin (43 kDa), and an $NH_2$-terminal fragment of the *P. falciparum* ORC1 protein (PfORC1N) (24 kDa) were also loaded as standards. The arrow indicates the position of both the wild-type and mutant proteins. (H) Size-exclusion chromatography of wild-type PfGyrB, PfGyrBN2, and PfGyrBN1 in the absence of ATP. Wild-type or deletion mutant proteins were passed through a Sepherose-12 gel filtration column, and 0.5-ml fractions were collected in each case. The fraction numbers are shown at the top. The elution patterns of the following gel filtration standards are indicated at the top: thyroglobulin (669 kDa), ferritin (440 kDa), catalase (232 kDa), aldolase (158 kDa), bovine serum albumin (66 kDa), ovalbumin (43 kDa), and chymotrypsinogen (25 kDa). In each case, a 60-μl sample was boiled in SDS-PAGE boiling buffer followed by SDS-PAGE analysis and Coomassie staining of the gels to obtain the elution patterns of wild-type and N-terminal deletion mutant proteins. Arrows facing upward indicate the positions of the peak fractions in each case. (I) Amino acid sequence of leucine heptad repeats of PfGyrA from positions 835 to 856. (J) Glutaraldehyde cross-linking of PfGyrACC. One microgram of protein was cross-linked with 0.001% glutaraldehyde in phosphate-buffered saline at 37°C for 15 min and subjected to SDS-PAGE followed by Western blot analysis using anti-$His_6$ polyclonal antibodies. BSA was also included in the reaction mixture as a control. PfGyrBC was used as a negative control for the cross-linking reaction.

anti-$His_6$ polyclonal antibodies. We observed that PfGyACC formed dimers as well as multimers, as shown in Fig. 6J. This dimerization is specific, since the addition of BSA does not change the nature of the cross-linked products, and a control protein, PfGyrBC, without leucine heptad repeats does not form dimers under the same experimental conditions. These results suggest that the unique leucine heptad repeats might be essential for the dimerization of PfGyrA.

## DISCUSSION

The presence of both subunits of gyrase in the *P. falciparum* genome, the inhibition of apicoplast DNA replication by ciprofloxacin, and the recent report of the characterization of the ATPase domain of *P. vivax* gyrase B provide circumstantial evidence for the presence of a functional gyrase in *Plasmodium* (10, 30, 55). Interestingly, other than prokaryotes, functional gyrase has been reported only in the plant *Arabidopsis thaliana* (51). Studies of *P. falciparum* gyrases that are potentially good targets for drugs have been limited due to the high AT content and differential codon usage of *Plasmodium*. Here, we report for the first time the cloning and functional biochemical characterization of PfGyr subunits that are targeted to the apicoplast.

As discussed above, the difficulties in the expression and purification of large *Plasmodium falciparum* proteins in the heterologous system might explain why there is no report in the literature regarding the expression and purification of >100-kDa *P. falciparum* proteins under normal conditions. Using several optimization/standardization procedures, we have been able to express and purify full-length PfGyrB as well as different functional domains of PfGyrA. We found that the incubation of bacterial cultures at lower temperatures (20 to 22.5°C), induction using low IPTG concentrations, and the use of the specialized *E. coli* strain BL21 Codon Plus, which can supply some of the rare codons (Arg, Ile, and Leu), might help to express high-molecular-mass *Plasmodium* proteins in *E. coli*. Interestingly, although we could express and purify the full-length PfGyrB protein, we were unable to express the full-length PfGyrA protein under the same experimental conditions. However, we could express and purify two functional domains of PfGyrA, and both domains were enzymatically active, suggesting that the purification of full-length PfGyrA is possible upon further optimization of the protocols.

RT-PCR analysis showed that the expression levels of PfGyrA and PfGyrB transcripts peak during the trophozoite and schizont stages. It was previously shown that apicoplast DNA replication coincides with nuclear DNA replication and that most of the DNA replication takes place during the late trophozoite and schizont stages. Therefore, the expression patterns of PfGyr subunits perfectly coincide with asexual DNA replication stages.

In *Plasmodium*, the gyrases are encoded in the nucleus and then carried to the apicoplast. Targeting of the gyrases to this organelle is consistent with the absence of any DNA replication gene found in the apicoplast genome. In *Arabidopsis*, separate GyrB proteins are targeted to the different organelles, like the chloroplast and mitochondria. *A. thaliana* GyrA has a dual translational initiation site targeting the mature protein to both the chloroplast and mitochondria (51). The genome of *Plasmodium falciparum* contains only one copy each of the *gyrA* and *gyrB* genes. It would be interesting to see whether these genes are targeted to mitochondria that contain ~6-kb linear DNA (11).

Pf*gyrB* complemented *E. coli gyrB* temperature-sensitive mutant cells at the restrictive temperature, whereas Pf*gyrA* failed to complement an *E. coli gyrA* temperature-sensitive strain. Later, we found that Pf*gyrA* was not expressed from plasmid pAD1, which was used to transform *E. coli gyrA* temperature-sensitive cells. The PfGyrA open reading frame did not contain any mutation, suggesting that the inability to express Pf*gyrA* in a heterologous system could be attributed to the inherent property of the gene. It is possible that some posttranslational modification of PfGyrA is required for its stability.

We observed intrinsic ATPase activity of full-length PfGyrB. The ATPase activity could be stimulated by the addition of EcGyrA or DNA that is the hallmark of the ATPase activity of gyrase. Significant ATPase activity has not been reported in the case of *E. coli* gyrase B, except for one study that reported appreciable intrinsic ATPase activity that was not stimulated by *E. coli* GyrA and/or DNA. *Mycobacterium smegmatis* GyrB also does not show intrinsic ATPase activity (31, 48). Those results suggest that PfGyrB is different from its *E. coli* counterpart.

Finally, in order to further investigate the differences in the ATPase activities of the *E. coli* and *P. falciparum* counterparts, we studied the rate of ATP hydrolysis with increasing full-length enzyme concentrations. With increasing enzyme concentrations, the ATP hydrolysis curve follows a linear pattern that is contrary to that of the *E. coli* enzyme, which follows a nonlinear curve of ATP hydrolysis (Fig. 4E and G). A comparison of the ATPase activities of ~43-kDa fragments of PfGyrB and EcGyrB further confirmed the linear rate of ATP hydrolysis in the case of PfGyrBN1 at higher enzyme concentrations. These results suggest that the enzyme kinetics of PfGyrB are truly different from those of its *E. coli* counterpart.

The activation of monomeric EcGyrB needs ATP-dependent dimerization, which accounts for the nonlinear rate of ATP hydrolysis with respect to the enzyme concentration. One obvious explanation for the apparent linear rate of ATP hydrolysis of PfGyrB is that dimerization is not necessary for ATP hydrolysis for PfGyrB. Alternatively, it is possible that PfGyrB exists as a stable dimer. The glutaraldehyde cross-linking experiments, native PAGE analysis, and gel filtration chromatography results confirm the latter hypothesis, since PfGyrB forms a stable dimer in the absence of ATP, whereas EcGyrB forms such dimers only in the presence of the ATP analogue drug coumermycin.

The dimerization of PfGyrB was not restricted to any single fragment. All fragments, including the full-length enzyme, showed dimers to be the preferred state in solution both by cross-linking experiments and by gel filtration chromatography in the absence of ATP. It is not very surprising that PfGyrBN2 eluted as dimers and also as high-molecular-mass forms, although PfGyrB (WT) and PfGyrBN1 eluted mostly as dimers only. Due to the smaller size of PfGyrBN2, this protein is always expressed in large quantities, and the yield is at least 5 to 10 times higher than those of the other forms of the proteins. It is possible that the very high level of expression of the proteins may push it to form higher-molecular-mass multi-

meric or aggregated forms of the protein. However, there is a definite pool of dimeric proteins, as shown in Fig. 6H.

These results for PfGyrB can be correlated to the ATP hydrolysis studies of *Saccharomyces cerevisiae* topoisomerase II. It was previously reported that the N terminus of yeast topoisomerase II (1 to 409 residues) without the dimerization domain shows a weak and nonlinear pattern of ATP hydrolysis, whereas a larger fragment including the dimerization domain (1 to 660 residues) shows a robust and linear pattern of ATP hydrolysis (36). Interestingly, the mutation of the Ile128 residue does not affect PfGyrB dimerization as it does for EcGyrB, suggesting that other amino acid residues are important for PfGyrB dimerization (6). Presently, we are trying to crystallize PfGyrBN2, which might shed some light on these ideas. Finally, the identification of unique leucine heptad repeats in PfGyrA leading to the dimerization/multimerization of this region is also a novel finding. The functional implication of this region in protein-protein or protein-DNA interactions needs to be explored further.

These results also raise an important question: if P*fgyrB* can dimerize in the absence of ATP, how can DNA segments (G or T segment) enter the gyrase active site if the N gate remains closed, as proposed by the model described previously by Wang based on the findings on yeast topoisomerase II (53)? Note that although the ATP-independent dimerization and linear rate of the ATP hydrolysis pattern of PfGyrB are unique for a gyrase enzyme, a similar result has been shown recently for the *Leishmania* topoisomerase II enzyme, where the "N"-terminal 43-kDa fragment shows ATP-independent dimerization and a linear pattern of the ATP hydrolysis rate, like PfGyrB (45). Together, these results suggest that these parasitic topoisomerase enzymes might have evolved in a different way, which needs to be studied in great detail to understand how the conventional model of the topoisomerase II "N" gate, which opens and closes in an ATP-dependent manner, can be extended to these unique systems. It is possible that these enzymes follow a unique mechanism, which is a broader issue and needs to be elucidated further.

The functional characterization of PfGyrB and the different functional domains of PfGyrA set the platform for a detailed biochemical and in vivo analysis of these enzymes, which are good targets for therapy. The results presented in this study lead to a simple model where two monomers of PfGyrB have the propensity to form stable dimers in solution due to the as-yet-unidentified dimer-forming interfaces (see Fig. S4 in the supplemental material). These dimers show a linear rate of ATP hydrolysis; the energy thus obtained can be used for DNA cleavage and DNA supercoiling activity together with PfGyrA. These data support the existence of a gyrase in the apicoplast of *P. falciparum*. It is likely that the apicoplast has retained a bacterium-type mechanism of DNA replication that requires gyrase for the maintenance of supercoiling in the organellar DNA.

## ACKNOWLEDGMENTS

This work is supported by the Wellcome Trust London. S.K.D. is a Wellcome Trust Senior International Research Fellow. N.M. acknowledges financial support from the UNICEF/UNDP/World Bank/WHO Special Programme for Research and Training in Tropical Diseases (TDR). M.A.D. acknowledges the University Grant Commission, India, for the fellowship.

We acknowledge V. Nagaraja (IISC, Bangalore) for providing the *E. coli* gyrase temperature-sensitive strains and purified Topo I enzyme for the relaxation assay and overall encouragement to carry out this project. A. Maxwell is acknowledged for plasmids pAG111 and pHH3. Ashish Gupta and Parul Mehra are acknowledged for their help with RT-PCR, immunofluorescence assay, and purified PfORC1N protein. We also acknowledge P. Sharma (National Institute of Immunology, New Delhi), Chetan Chitnis and Nirupam Roy Choudhury (ICGEB, New Delhi), Samudrala Gourinath and Neelima Alam (SLS, JNU), Anindya Dutta (University of Virginia), and Gauranga Mukhopadhyay (SCMM, JNU) for reagents and fruitful discussions.

## REFERENCES

1. **Ali, J. A., A. P. Jakson, A. J. Howells, and A. Maxwell.** 1993. The 43-kilodalton N-terminal fragment of the DNA gyrase B protein hydrolyzes ATP and binds coumarin drugs. Biochemistry **32:**2717–2724.
2. **Anquetin, G., J. Greiner, N. Mahmoudi, M. Santillana-Hayat, R. Gozalbes, K. Farhati, F. Derouin, A. Aubry, E. Cambau, and P. Vierling.** 22 September 2006. Design, synthesis and activity against Toxoplasma gondii, Plasmodium spp., and Mycobacterium tuberculosis of new 6-fluoroquinolones. Eur. J. Med. Chem. **41:**1478–1493. [Epub ahead of print.]
3. **Anquetin, G., J. Greiner, and P. Vierling.** 2005. Quinolone-based drugs against Toxoplasma gondii and Plasmodium spp. Curr. Drug Targets Infect. Disord. **5:**227–245.
4. **Arvind, L., L. M. Iyer, T. E. Wellems, and L. H. Miller.** 2003. Plasmodium biology: genomic gleanings. Cell **115:**771–785.
5. **Bozdech, Z., M. Llinas, B. L. Pulliam, E. D. Wong, J. Zhu, and J. L. DeRisi.** 2003. The transcriptome of the intraerythrocytic developmental cycle of Plasmodium falciparum. PLoS Biol. **1:**E5.
6. **Brino, L., A. Urzhumtsev, M. Mousli, C. Bronner, A. Mitschler, P. Oudet, and D. Moras.** 2000. Dimerization of Escherichia coli DNA-gyrase B provides a structural mechanism for activating the ATPase catalytic center. J. Biol. Chem. **275:**9468–9475.
7. **Brown, P. O., C. L. Peebles, and N. R. Cozzaarelli.** 1979. A topoisomerase from Escherichia coli related to DNA gyrase. Proc. Natl. Acad. Sci. USA **76:**6110–6114.
8. **Champoux, J. J.** 2001. DNA topoisomerases: structure, function, and mechanism. Annu. Rev. Biochem. **70:**369–413.
9. **Chatterji, M., S. Unniraman, A. Maxwell, and V. Nagaraja.** 2000. The additional 165 amino acids in the B protein of Escherichia coli DNA gyrase have an important role in DNA binding. J. Biol. Chem. **275:**22888–22894.
10. **Chavalitshewinkoon-Petmitr, P., R. Worasing, and P. Wilairat.** 2001. Partial purification of mitochondrial DNA topoisomerase II from Plasmodium falciparum and its sensitivity to inhibitors. Southeast Asian J. Trop. Med. Public Health **32:**733–738.
11. **Conway, D. J., C. Fanello, J. M. Lloyd, B. M. Al-Joubori, A. H. Baloch, S. D. Somanath, C. Roper, A. M. Oduola, B. Mulder, M. M. Povoa, B. Singh, and A. W. Thomas.** 2000. Origin of Plasmodium falciparum malaria is traced by mitochondrial DNA. Mol. Biochem. Parasitol. **111:**163–171.
12. **Corbett, K. D., and J. M. Berger.** 2004. Structure, molecular mechanisms, and evolutionary relationships in DNA topoisomerases. Annu. Rev. Biophys. Biomol. Struct. **33:**95–118.
13. **Dao-Thi, M. H., L. V. Melderen, E. D. Genst, H. Afif, L. But, L. Wyns, and R. Loris.** 2005. Molecular basis of gyrase poisoning by the addiction toxin CcdB. J. Mol. Biol. **348:**1091–1102.
14. **Dao-Thi, M. H., L. Van Melderen, E. D. Genst, L. Buts, A. Ranquin, L. Wyns, and R. Loris.** 2004. Crystallization of CcdB in complex with a GyrA fragment. Acta Crystallogr. D **60:**1132–1134.
15. **Divo, A. A., A. C. Sartorelli, C. L. Patton, and F. J. Bia.** 1988. Activity of fluoroquinolone antibiotics against *Plasmodium falciparum* in vitro. Antimicrob. Agents Chemother. **32:**1182–1186.
16. **Drlica, L., and X. Zhao.** 1997. DNA gyrase, topoisomerase IV, and the 4-quinolones. Microbiol. Mol. Biol. Rev. **61:**377–392.
17. **Fichera, M. E., and D. S. Roos.** 1997. A plastid organelle as a drug target in apicomplexan parasites. Nature **390:**407–409.
18. **Foth, B. J., and G. I. McFadden.** 2003. The apicoplast: a plastid in Plasmodium falciparum and other apicomplexan parasites. Int. Rev. Cytol. **224:**57–110.
19. **Foth, B. J., S. A. Ralph, C. J. Tonki, N. S. Struck, M. Fruanholz, D. S. Roos, A. F. Cowman, and G. I. McFadden.** 2003. Dissecting apicoplast targeting in the malaria parasite *Plasmodium falciparum*. Science **299:**705–707.
20. **Gardner, M. J., N. Hall, E. Fung, O. White, M. Berriman, R. W. Hyman, J. M. Carlton, A. Pain, et al.** 2002. Genome sequence of the human malaria parasite Plasmodium falciparum. Nature **419:**498–511.
21. **Gellert, M., L. M. Fisher, and M. H. O'Dea.** 1979. DNA gyrase: purification and catalytic properties of a fragment of gyrase B protein. Proc. Natl. Acad. Sci. USA **76:**6289–6293.
22. **Gellert, M., K. Mizuuchi, M. H. O'Dea, and H. A. Nash.** 1976. DNA gyrase: an enzyme that introduces superhelical turns into DNA. Proc. Natl. Acad. Sci. USA **73:**3872–3876.
23. **Gormley, N. A., G. Orphanides, A. Meyer, P. M. Cullis, and A. Maxwell.**

1996. The interaction of coumarin antibiotics with fragments of DNA gyrase B protein. Biochemistry **35:**5083–5092.
24. **Gritzmacher, C. A., and R. T. Reese.** 1984. Protein and nucleic acid synthesis during synchronized growth of *Plasmodium falciparum*. J. Bacteriol. **160:** 1165–1167.
25. **Hadi, S. A., T. A. Bickle, and R. Yuan.** 1975. The role of S-adenosylmethionine in the cleavage of deoxyribonucleic acid by the restriction endonuclease from Escherichia coli K. J. Biol. Chem. **250:**4159–4164.
26. **Hallet, P., A. J. Grimshaw, D. B. Wigley, and A. Maxwell.** 1990. Cloning of the DNA gyrase genes under tac promoter control: overproduction of the gyrase A and B proteins. Gene **93:**139–142.
27. **Harlow, E., and D. Lane.** 1988. Antibodies. Cold Spring Harbor Laboratory Press, Cold Spring Harbor, NY.
28. **Inselberg, J., and H. S. Banyal.** 1984. Synthesis of DNA during the asexual cycle of Plasmodium falciparum in culture. Mol. Biochem. Parasitol. **10:** 79–87.
29. **Jackson, A. P., and A. Maxwell.** 1993. Identifying the catalytic residue of the ATPase reaction of DNA gyrase. Proc. Natl. Acad. Sci. USA **90:**11232–11236.
30. **Khor, V., C. Yowell, J. B. Dame, and T. C. Rowe.** 2005. Expression and characterization of the ATP-binding domain of a malarial Plasmodium vivax gene homologous to the B-subunit of the bacterial topoisomerase DNA gyrase. Mol. Biochem. Parasitol. **140:**107–117.
31. **Manjunatha, U. H., M. Dalal, M. Chatterji, D. R. Radha, S. S. Visweswariah, and V. Nagaraja.** 2002. Functional characterisation of mycobacterial DNA gyrase: an efficient decatenase. Nucleic Acids Res. **30:**2144–2153.
32. **Maxwell, A.** 1997. DNA gyrase as a drug target. Trends Microbiol. **5:**102–109.
33. **Maxwell, A., and M. Gellert.** 1984. The DNA dependence of the ATPase activity of DNA gyrase. J. Biol. Chem. **289:**14472–14480.
34. **Mehra, P., A. K. Biswas, A. Gupta, S. Gourinath, C. E. Chitnis, and S. K. Dhar.** 2005. Expression and characterization of human malaria parasite Plasmodium falciparum origin recognition complex subunit 1. Biochem. Biophys. Res. Commun. **337:**955–966.
35. **Oh, Y. L., B. Hamim, Y. K. Kim, H. K. Lee, J. W. Lee, O. K. Song, K. Tsukiyama-Kohara, M. Kohara, A. Nomoto, and S. K. Jang.** 1998. Determination of functional domains in polypyrimidine-tract-binding protein. Biochem. J. **331:**169–175.
36. **Olland, S., and J. C. Wang.** 1999. Catalysis of ATP hydrolysis by two NH(2)-terminal fragments of yeast DNA topoisomerase II. J. Biol. Chem. **274:** 21688–21694.
37. **Pizzi, E., and C. Frontali.** 2001. Low-complexity regions in Plasmodium falciparum proteins. Genome Res. **11:**218–229.
38. **Rajos, M. O. D., and M. Wesserman.** 1985. Temporal relationships on macromolecular synthesis during the asexual cell cycle of Plasmodium falciparum. Trans R. Soc. Trop. Med. Hyg. **79:**792–796.
39. **Ralph, S. A., B. J. Foth, N. Hall, and G. I. McFadden.** 2004. Evolutionary pressures on apicoplast transit peptides. Mol. Biol. Evol. **21:**2183–2194.
40. **Ralph, S. A., G. G. Vandoren, R. F. Waller, and G. I. McFadden.** 2004. Tropical infectious diseases: metabolic maps and functions of the Plasmodium falciparum apicoplast. Nat. Rev. Microbiol. **2:**203–216.
41. **Reece, R. J., and A. Maxwell.** 1989. Tryptic fragments of the Escherichia coli DNA gyrase A protein. J. Biol. Chem. **264:**19448–19453.
42. **Reece, R. J., and A. Maxwell.** 1991. The C-terminal domain of the Escherichia coli DNA gyrase A subunit is a DNA-binding protein. Nucleic Acids Res. **19:**1399–1405.
43. **Roos, D. S., M. J. Crawford, R. G. K. Donald, M. Fraunholz, O. S. Harb, C. Y. He, J. C. Kissinger, M. K. Shaw, and B. Striepen.** 2002. Mining the Plasmodium genome database to define organellar function: what does the apicoplast do? Philos. Trans. R. Soc. Lond. **357:**35–46.
44. **Sambrook, J., E. F. Fritsch, and T. Maniatis.** 1989. Molecular cloning: a laboratory manual, 2nd ed. Cold Spring Harbor Laboratory Press, Cold Spring Harbor, NY.
45. **Sengupta, T., M. Mukherjee, A. Das, C. Mandal, R. Das, T. Mukherjee, and H. K. Majumder.** 2005. Characterization of the ATPase activity of topoisomerase II from Leishmania donovani and identification of residues conferring resistance to etoposide. Biochem. J. **390:**419–426.
46. **Simon, H., M. Roth, and C. Zimmer.** 1995. Biochemical complementation studies in vitro of gyrase subunits from different species. FEBS Lett. **373:** 88–92.
47. **Smith, C. V., and A. Maxwell.** 1998. Identification of a residue involved in transition-state stabilization in the ATPase reaction of DNA gyrase. Biochemistry **37:**9658–9667.
48. **Staudenbauer, W. L., and E. Orr.** 1981. DNA gyrase: affinity chromatography on novobiocin-Sepharose and catalytic properties. Nucleic Acids Res. **9:**3589–3603.
49. **Su, X.-Z., Y. Wu, D. C. Sifri, and T. E. Wellems.** 1996. Reduced extension temperatures required for PCR amplification of extremely A+T-rich DNA. Nucleic Acids Res. **24:**1574–1575.
50. **Sugino, A., and N. R. Cozzarelli.** 1980. The intrinsic ATPase of DNA gyrase. J. Biol. Chem. **255:**6299–6306.
51. **Wall, M. K., L. A. Mitchenal, and A. Maxwell.** 2004. Arabidopsis thaliana DNA gyrase is targeted to chloroplasts and mitochondria. Proc. Natl. Acad. Sci. USA **101:**7821–7826.
52. **Waller, R. F., P. J. Keeling, R. G. K. Donald, B. Striepen, E. Handman, N. Lang-Unnasch, A. F. Cowman, G. S. Besra, D. S. Roos, and G. I. McFadden.** 1998. Nuclear-encoded proteins target to the plastid in Toxoplasma gondii and Plasmodium falciparum. Proc. Natl. Acad. Sci. USA **95:**12352–12357.
53. **Wang, J. C.** 1998. Moving one DNA double helix through another by a type II DNA topoisomerase: the story of simple molecular machine. Q. Rev. Biophys. **31:**107–144.
54. **Waters, N. C., K. M. Kopydlowski, T. Guszczynski, L. Wei, P. Sellers, J. T. Ferlan, P. J. Lee, Z. Li, C. L. Woodard, S. Shallom, M. J. Gardner, and S. T. Prigge.** 2002. Functional characterization of the acyl carrier protein (PfACP) and beta-ketoacyl ACP synthase III (PfKASIII) from Plasmodium falciparum. Mol. Biochem. Parasitol. **123:**85–94.
55. **Weissig, V., T. S. Vetro-Widenhouse, and T. C. Rowe.** 1997. Topoisomerase II inhibitors induce cleavage of nuclear and 35-kb plastid DNAs in the malarial parasite Plasmodium falciparum. DNA Cell Biol. **16:**1483–1492.
56. **Williamson, D. H., P. R. Preiser, P. W. Moore, S. McCready, M. Strath, and R. J. M. Wilson.** 2002. The plastid DNA of the malaria parasite *Plasmodium falciparum* is replicated by two mechanisms. Mol. Microbiol. **45:**533–545.
57. **Williamson, D. H., P. R. Preiser, and R. J. M. Wilson.** 1996. Organelle DNAs: the bit players in malaria parasite DNA replication. Parasitol. Today **12:**357–362.
58. **Wilson, R. J.** 2002. Progress with parasite plastids. J. Mol. Biol. **319:**257–274.
59. **Wilson, R. J., and D. H. Williamson.** 1997. Extrachromosomal DNA in the Apicomplexa. Microbiol. Mol. Biol. Rev. **61:**1–16.
60. **Zeng, X., A. M. Herndon, and J. C. Hu.** 1997. Buried asparagines determine the dimerization specificities of leucine zipper mutants. Proc. Natl. Acad. Sci. USA **94:**3673–3678.